

Ab-initio Study of Magnetically Intercalated Tungsten Diselenide

Peter D. Reyntjens^{1,2,3}, Sabyasachi Tiwari^{1,2,3}, Maarten L. Van de Put¹,
Bart Sorée^{2,4,5} and William G. Vandenberghe¹

¹ Department of Materials Science and Engineering, The University of Texas at Dallas,
800 W Campbell Rd., Richardson, Texas 75080, USA.

² Imec, Kapeldreef 75, 3001 Heverlee, Belgium.

³ Department of Materials Engineering, KU Leuven,
Kasteelpark Arenberg 44, 3001 Leuven, Belgium.

⁴ Department of Electrical Engineering, KU Leuven,
Kasteelpark Arenberg 10, 3001 Leuven, Belgium.

⁵ Department of Physics, Universiteit Antwerpen, Groenenborgerlaan 171, 2020 Antwerp, Belgium.

Abstract—We theoretically investigate the effect of intercalation of third row transition metals (Co, Cr, Fe, Mn, Ti and V) in the layers of WSe₂. Using density functional theory (DFT), we investigate the structural stability. We also compute the DFT energies of various magnetic spin configurations. Using these energies, we construct a Heisenberg Hamiltonian and perform a Monte Carlo study on each WSe₂ + intercalant system to estimate the Curie or Néel temperature. We find ferromagnetic ground states for Ti and Cr intercalation, with Curie temperatures of 31K and 225K, respectively. In Fe-intercalated WSe₂, we predict that antiferromagnetic ordering is present up to 564K. For V intercalation, we find that the system exhibits a double phase transition.

I. INTRODUCTION

Transition metal dichalcogenides (TMDs) which contain heavy elements such as tungsten (W) have attracted significant attention for their exceptional electronic properties [1], and their potential applications in spintronics [2]. The properties of TMDs can be enhanced or modified using dopants, further increasing their scope of potential applications.

An interesting field is that of spintronics, where magnetic materials are used to control the flow of information [2]. There are several ways of obtaining magnetism in TMDs. Some TMDs exhibit intrinsic magnetism in their monolayer form, for example VSe₂ [3]. Doping TMDs with magnetic transition metals as substitutional dopants [4] or as intercalants [5], is the most promising method of realizing TMDs which retain magnetic order up to room temperature.

In this work, we calculate the Curie or Néel temperatures of WSe₂, intercalated with the third-row transition metals Ti, V, Cr, Mn, Fe and Co. We use density functional theory (DFT) to find the optimal structures and the total energies of a set of spin-polarized states for each material. Next, we simulate the magnetic behavior for finite temperature using Monte Carlo simulations. We report the Curie (Néel) temperature for each (anti)ferromagnetic material. To assess the thermodynamic stability of the materials we study, we compute the formation energy for each host-dopant combination.

II. COMPUTATIONAL METHODS

Figure 1 shows a flowchart of the simulation process we use in this work. In all our DFT calculations, we employ an energetic plane-wave cut-off of 500 eV. We employ a Gamma-centered k-point grid, which we vary according to the supercell size.

The DFT simulations are performed using the Vienna *ab initio* Simulation Package (VASP) [6]. We use the Perdew-Burke-Ernzerhof (PBE) functional based on the generalized gradient approximation [7]. We consider the van der Waals interactions by using the DFT-D3 corrections of Grimme *et al.* [8]. We then calculate the Hubbard U parameter using the linear response method [9].

A. Structural relaxation

Figure 2 shows the structures we use in our work. We first use DFT to find the optimal atomic positions and lattice parameters. We intercalate into a $2 \times 2 \times 2$ supercell of WSe₂ where we place two transition metal dopant atoms above each other, but between different WSe₂ layers.

We perform the structural relaxation until the forces on the atoms are all below 5×10^{-3} eV/Å, using a $6 \times 6 \times 4$ k-grid.

B. Hubbard U

In 3d transition metals, the d -shell electrons are strongly correlated. To correctly calculate the properties of the system, we employ the Hubbard U -corrected DFT+ U . We calculate the value of the Hubbard U parameter using the linear response technique of S. de Gironcoli and M. Cococcioni [9]. Once we have the value for the Hubbard U for each host-dopant combination, we proceed with the spin-polarized DFT+ U calculations.

C. Magnetic states

We calculate the magnetic properties of the materials using collinear DFT within the collinear approximation. We simulate

the unique magnetic states in the supercell by applying a positive or negative magnetic moment to each intercalant atom. To find the unique magnetic states, we first consider all possible magnetic states in the supercell and then remove symmetry-equivalent states. Later, in the Monte Carlo calculations, we take into account the multiplicity of the states.

In the spin-polarized calculations, we place the magnetic moments on each of the intercalant atoms, while leaving the host-TMD atoms unpolarized, with an initial magnetic moment of $0\mu_B$. For the initial magnetic moment on the intercalant atoms, we use the number of unpaired electrons in the d -shell of the dopant atom, times the Bohr magneton. This corresponds to an initial magnetic moment of $2\mu_B$ for Ti, $3\mu_B$ for Co and V, $4\mu_B$ for Fe and finally $5\mu_B$ for Cr and Mn. For the spin-polarized DFT calculations, we use a $4 \times 2 \times 2$ supercell, with four intercalant atoms. The k-point grid is a Gamma-centered $3 \times 6 \times 4$ grid.

To determine the temperature at which the system transitions between an ordered magnetic state and a disordered state, we calculate the magnetic susceptibility and specific heat from the results of our Monte Carlo runs. We take the peak of the specific heat as the phase transition temperature, namely the Curie temperature for ferromagnets and the Néel temperature for antiferromagnets.

D. Heisenberg Hamiltonian

To model the magnetic interactions, we employ a $J_1 - J_2$ model where J_1 is the in-plane interaction between in-plane nearest neighbors, while J_2 contains the out-of-plane nearest-neighbor interaction. We obtain the values of the exchange parameters using the parametrization scheme described in Refs. [10], [11]. After estimating the exchange parameters, we plug them into a classical Heisenberg Hamiltonian, where the positions of the intercalant atoms correspond to the magnetic sites in the model.

E. Monte Carlo simulations

For the Monte Carlo calculations, we employ a supercell consisting solely of the intercalant atoms, serving as magnetic sites in our model, with $9 \times 9 \times 8$ atoms. For each temperature step, we perform 2000 equilibration steps and 2000 Monte Carlo steps. Additionally, we run each simulation six times, each time starting from a different random initial magnetic configuration, and average the results over the six runs.

F. Formation energies

We calculate the formation energies of the various intercalated materials from the DFT total energies after relaxation. The formation energy of the material is calculated as

$$E_{\text{form}} = \frac{1}{N_1} (E_{\text{intercalated}} - N_1 E_{\text{pure}} - N_2 E_{\text{dopant}}) \quad (1)$$

where N_1 is the number of WSe₂ unit cells in the supercell, while N_2 is the number of dopant atoms per supercell. $E_{\text{intercalated}}$ is the DFT total energy of the intercalated WSe₂ supercell. E_{pure} is the DFT total energy of the WSe₂ unit cell, without intercalants. Finally, E_{dopant} is the DFT total energy of a dopant atom in its bulk metallic form.

A. Crystal structure optimization

Figure 2 shows the structures we use in our work. We intercalated third-row transition metal atoms, namely Ti, V, Cr, Mn, Fe and Co, between the layers of WSe₂. In a first step, we start from the 2H AB stacked structure shown in Figs 2a and 2b for all intercalants. However, after the relaxations, we find that the distorted Bernal structure, shown in Figs. 2c and 2d, is more stable than the 2H AB structure for Ti, V, Cr and Mn intercalation. We use the distorted Bernal structure for all subsequent calculations involving X-intercalated WSe₂, where X = Ti, V, Cr, Mn. In the case of Fe and Co intercalation, we use the 2H AB structure for the subsequent calculations.

B. Magnetic states

Table I shows the values we obtain during the next steps in our workflow. We report the in-plane and out-of-plane exchange parameters, the Hubbard U parameter calculated using linear response, the final magnetic moment on the intercalant atoms and the estimated transition temperature, obtained from our Monte Carlo simulations. For Ti and Cr, DFT calculations predict a ferromagnetic ground state, while the most stable DFT state for V, Mn, Fe and Co intercalation is antiferromagnetic.

For each host-dopant combination we use the $J_1 - J_2$ model, with an in-plane and an out-of-plane interaction term. In the ferromagnetic materials, Ti and Cr-doped WSe₂, both exchange parameters are positive, indicating ferromagnetic in-plane and out-of-plane interactions. For Mn, the two exchange parameters are negative indicating purely antiferromagnetic interactions. Whereas V, Fe and Co-intercalated WSe₂ show ferromagnetic out-of-plane and antiferromagnetic in-plane interactions.

Figure 3 shows the susceptibility curves of the intercalated WSe₂ versus temperature. For each material, we divide the susceptibility by its maximum value, to normalize the curves for a better comparison of the different materials.

Figure 4 shows the specific heat curves for the intercalated WSe₂. We again normalize the curves for better comparison, by dividing each one by its maximum value. The transition temperatures reported in Table I are the locations of the specific heat peaks.

In Fig. 5, we plot the average magnetization and the specific heat of V-intercalated WSe₂ versus temperature. We see a cusp in the specific heat, at a somewhat lower temperature than the main peak. We see that the magnetization exhibits a rather complex structure. The peaks in the specific heat occur at the same temperature as abrupt changes in the magnetization, which are caused by distinct phase transitions. There are two such phase transitions, one at 118K and one at 36K. When cooling down from high temperature, the system undergoes a first phase transition at 118K, where some magnetic order appears. Upon further cooling, the system undergoes a second phase transition at 36K, where it transitions into its low-temperature antiferromagnetic ground state.

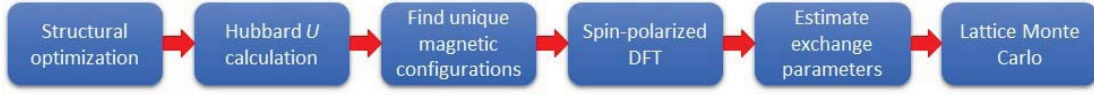


Fig. 1: Flowchart for our calculations. We perform a structural optimization, followed by a linear response calculation of the Hubbard U . After finding the unique spin configurations of the unit cell, we calculate the total energies which we use to calculate the magnetic exchange parameters. Finally, we calculate the Curie or Néel temperature by means of a lattice Monte Carlo simulation.

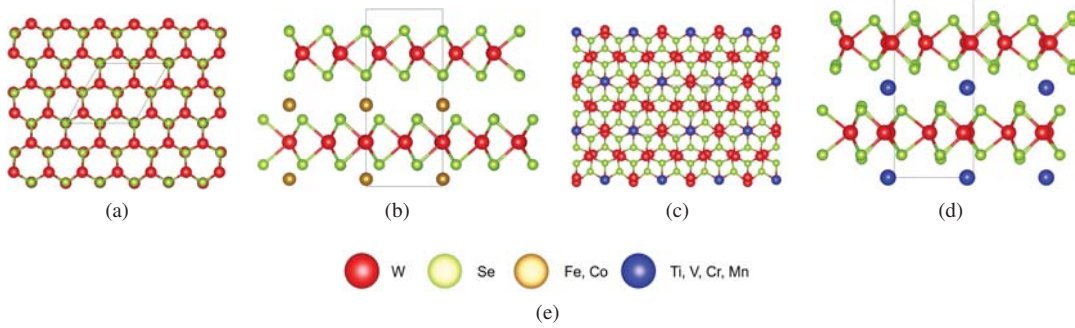


Fig. 2: (a) 2H AB structure for the intercalated WSe_2 , viewed from the out-of-plane direction. (b) 2H AB structure for the intercalated WSe_2 , viewed from the in-plane direction. For all intercalants, we start the structural optimization from this structure. For Fe and Co, we use the 2H AB structure for the spin-polarized DFT calculations. (c) Distorted Bernal structure for intercalated WSe_2 , viewed from the out-of-plane direction and (d) viewed from the in-plane direction. For Ti, V, Cr and Mn intercalation, the distorted Bernal structure is more stable than the 2H AB structure, and we use it for the spin-polarized DFT calculations.

		WSe_2					
Intercalant		Ti	V	Cr	Mn	Fe	Co
J_1 (meV)		0.255	-0.247	0.0658	-0.0307	-0.0362	-0.0482
J_2 (meV)		0.0332	0.361	0.207	-0.0136	4.08	3.08
Hubbard U (eV)		4.64	3.87	4.82	7.08	5.51	5.05
Magnetic moment		$1.76\mu_B$	$2.75\mu_B$	$4.11\mu_B$	$4.48\mu_B$	$2.64\mu_B$	$1.15\mu_B$
T_C		34K	—	225K	—	—	—
T_N		—	118K	—	88K	564K	40K

TABLE I: For each host-dopant combination, the results of our DFT and Monte Carlo calculations. We calculate the Hubbard U using the linear response method. The exchange parameters in the $J_1 - J_2$ model are J_1 , the interaction between in-plane nearest neighbors, and J_2 , the interaction between out-of-plane nearest neighbors. Finally, we report the transition temperatures calculated using our Monte Carlo simulations.

C. Formation energies

Figure 6 shows the formation energies for the materials we study. The formation energies are positive for all cases, indicating poor stability. We see that the formation energy is highest for Cr intercalation, and lowest for Ti intercalation. The formation energy is proportional the number of unpaired valence electrons in the d -shell of the intercalants; Cr and Mn have 5 unpaired electrons, while Ti only has 2.

IV. CONCLUSIONS

We have calculated the magnetic properties of WSe_2 intercalated with the third-row transition metals Ti, V, Cr, Mn, Fe

and Co. After structural optimization, we have calculated the total energies of different magnetic states in each system. The calculation of the in-plane and out-of-plane nearest neighbor exchange parameters reveals a few important facts. For Ti and Cr intercalation, the combined system has ferromagnetic nearest neighbor interactions, both in and out of plane, which corresponds to a ferromagnetic ground state at low temperature. In the case of Mn intercalation, the nearest-neighbor interactions are purely antiferromagnetic. The other three cases, *i.e.*, V, Fe and Co intercalation, have in-plane antiferromagnetic interactions and out-of-plane ferromagnetic interactions.

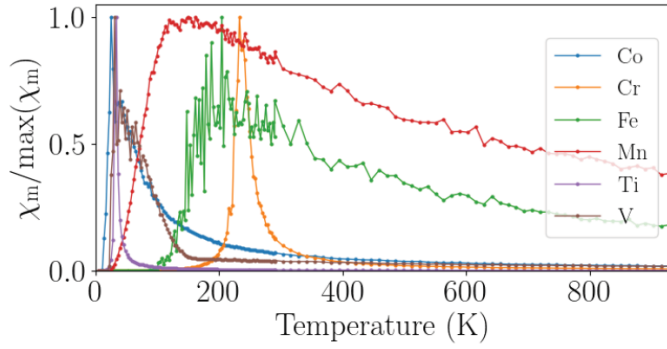


Fig. 3: The susceptibilities for WSe_2 intercalated with Ti, V, Cr, Mn, Fe and Co. We normalize the curves by dividing each one by its maximum value, in order to better compare the peaks.

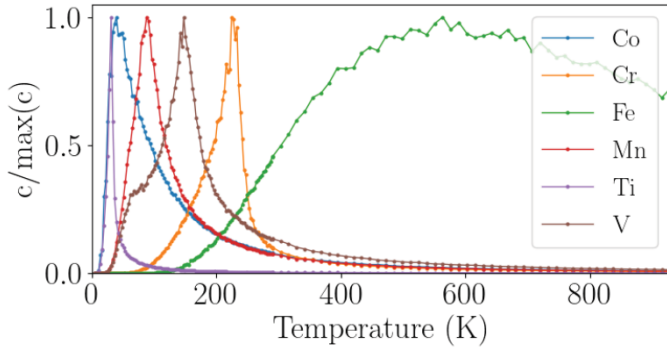


Fig. 4: The specific heat for WSe_2 intercalated with Ti, V, Cr, Mn, Fe and Co. For a better comparison between the different curves, we normalize them dividing them by their respective maximum values.

The specific heat curve of V-intercalated WSe_2 shows a double-peak structure, with a large peak at 118K and a cusp at 36K. The average magnetization of the system exhibits similar behavior, which we attribute to the existence of two phase transitions in the material.

While the formation energies of the materials studied here turn out to be positive, indicating poor stability, the results from the Monte Carlo simulations are encouraging. The magnetic behavior is very dependent on which atomic type is used to induce magnetism. In particular, the high transition temperature of Fe-intercalated WSe_2 and the double phase transition in V-intercalated WSe_2 are intriguing. More research into intercalated WSe_2 and other TMDs is necessary and may lead to extremely useful applications in the future.

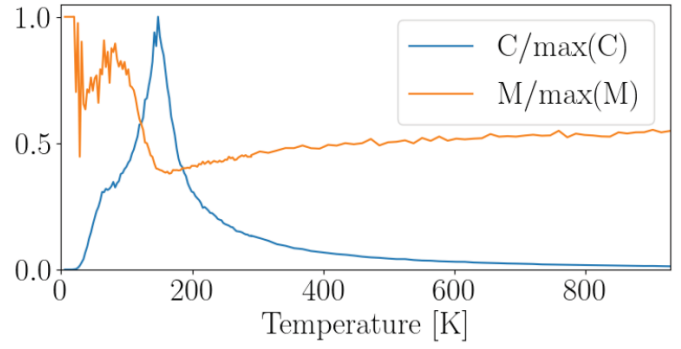


Fig. 5: The specific heat and magnetization for V-intercalated WSe_2 . The specific heat exhibits a double-peak structure, with a large peak at 118K and a smaller one at 36K. Each peak corresponds to a distinct phase transition. The two phase transitions are visible in the magnetization curve as well.

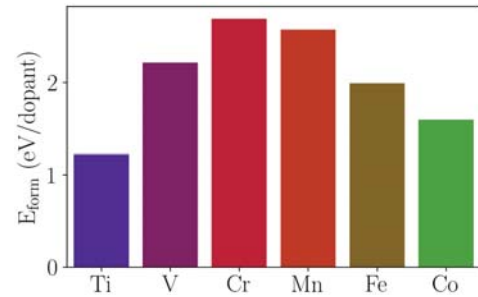


Fig. 6: The formation energies per intercalant for intercalated WSe_2 . Cr-intercalated WSe_2 has the highest formation energy, while Ti-intercalated WSe_2 has the lowest formation energy.

REFERENCES

- [1] Q. H. Wang, K. Kalantar-Zadeh, A. Kis, J. N. Coleman, and M. S. Strano, "Electronics and optoelectronics of two-dimensional transition metal dichalcogenides."
- [2] I. Žutić, J. Fabian, and S. Das Sarma, "Spintronics: Fundamentals and applications," *Rev. Mod. Phys.*, vol. 76, pp. 323–410, Apr 2004.
- [3] M. Bonilla, S. Kolekar, Y. Ma, H. C. Diaz, V. Kalappattil, R. Das, T. Eggers, H. R. Gutierrez, M.-H. Phan, and M. Batzill, "Strong room-temperature ferromagnetism in VSe_2 monolayers on van der waals substrates."
- [4] B. Li, T. Xing, M. Zhong, L. Huang, N. Lei, J. Zhang, J. Li, and Z. Wei, "A two-dimensional Fe-doped SnS_2 magnetic semiconductor."
- [5] Y. Jung, Y. Zhou, and J. J. Cha, "Intercalation in two-dimensional transition metal chalcogenides."
- [6] G. Kresse and J. Furthmüller, "Efficient iterative schemes for ab initio total-energy calculations using a plane-wave basis set," *Phys. Rev. B*, vol. 54, pp. 11 169–11 186, Oct 1996.
- [7] J. P. Perdew, K. Burke, and M. Ernzerhof, "Generalized gradient approximation made simple," *Phys. Rev. Lett.*, vol. 77, pp. 3865–3868, Oct 1996.
- [8] S. Grimme, J. Antony, S. Ehrlich, and H. Krieg, "A consistent and accurate ab initio parametrization of density functional dispersion correction (DFT-D) for the 94 elements H-Pu."
- [9] M. Cococcioni and S. de Gironcoli, "Linear response approach to the calculation of the effective interaction parameters in the LDA + U method," *Phys. Rev. B*, vol. 71, p. 035105, Jan 2005.
- [10] S. Tiwari, M. L. van de Put, B. Sorée, and W. G. Vandenberghe, "Magnetism of 2D semiconductors, dichalcogenides and graphene," in *Bulletin of the American Physical Society*, vol. 65, no. 1, 2020.
- [11] S. Tiwari, M. L. V. de Put, B. Soree, and W. G. Vandenberghe, "Critical behavior of ferromagnets CrI_3 , CrBr_3 , CrGeTe_3 , and anti-ferromagnet FeCl_2 : a detailed first-principles study," 2020.